Journal of Power Sources 196 (2011) 10532–10537

Contents lists available at ScienceDirect

Journal of Power Sources

journal homepage: www.elsevier.com/locate/jpowsour

High performance quasi-solid-state dye-sensitized solar cells based on poly(lactic acid-co-glycolic acid)

Woosung Kwon, Shi-Woo Rhee*

System on Chip Chemical Process Research Center, Department of Chemical Engineering, Pohang University of Science and Technology (POSTECH), Pohang 790-784, Republic of Korea

ARTICLE INFO

Article history:
Received 29 June 2011
Received in revised form 10 August 2011
Accepted 10 August 2011
Available online 17 August 2011

Keywords:
Polymer gel electrolytes
Dye-sensitized solar cells
Poly(lactic acid-co-glycolic acid)
Amphiphilic

ABSTRACT

A stable quasi-solid-state dye-sensitized solar cell (DSC) with a novel amphiphilic polymer gel electrolyte (APGE) based on poly(lactic acid-co-glycolic acid) (PLGA) is fabricated. The APGE could be readily prepared by a simple method at low temperature of 50 °C and exhibits a quasi-solid property, high conductivity, and long-term stability. The 20 and 40 wt% APGE-based DSCs show high photovoltaic conversion efficiency of 7.5 and 7.4%, respectively, under AM 1.5 simulated sunlight, which is comparable to the liquid electrolyte-based DSC with the efficiency of 7.6%. The 40 wt% APGE-based DSC maintains 95% of the initial performance after 60 days in practical conditions. It is also noteworthy that the APGE endows with higher short-circuit current density than the liquid electrolyte. Different natures of the APGE from the typical polymer gel electrolytes have been elucidated by the *I–V* measurements, electrochemical impedance spectroscopy, electrophoretic measurements, and transmission electron microscopy.

1. Introduction

Dye-sensitized solar cells (DSCs), first introduced by O'Regan and Grätzel in 1991, opened completely new prospects for photovoltaic devices [1]. Due to relatively low fabrication cost and the high photovoltaic conversion efficiencies, they have received considerable attention as a promising alternative for conventional solar cells. Typical DSCs are built up with three major compartments; a mesoporous nanocrystalline TiO_2 film sensitized by a dye for light harvesting, a redox mediator for dye-regeneration, and a platinized counter electrode for reduction of the redox couple. Photoexcited electron injection from the dyes into the conduction band of the TiO_2 film initiates charge separation driven by the potential difference between them [2]. The redox couple subsequently regenerates the oxidized dye and conveys the resulting holes to the counter electrode to be reduced. It is reported by Grätzel et al. [3] that DSCs with liquid electrolytes of the I_3^-/I^- redox couple have already attained a high photovoltaic conversion efficiencies of 11%. However, the presence of liquid solvents may cause substantial problems with long-term operation and robust sealing, which hampers large-scale outdoor applications of DSCs. Thus, solid-state and quasi-solid-state electrolytes such as polymer gel electrolytes [4–10], organic and inorganic hole-transporting materials [11–17], ionic liquids [18–22], and polymer electrolytes [23–28] have been suggested in order to replace the liquid electrolyte and guarantee long-term stability. Among the alternative electrolytes, polymer gel electrolytes (PGEs) could mitigate the leakage by retaining solvent molecules in the polymer matrices through immobilization and plasticization of organic solvents. Because of their gel characteristic, PGEs typically show high ionic conductivity comparable to the liquid electrolyte, reasonable permeability into the inner structure of the TiO_2 film, and negligible vapor pressure. In the past, however, most PGEs have low polymer content less than 20 wt% in order to attain reasonable ionic conductivities [29], and a large amount of the solvent cannot be retained.

In this paper, poly(lactic acid-co-glycolic acid) (PLGA) was incorporated into a acetonitrile-based liquid electrolyte in order to obtain a quasi-solid-state electrolyte. PLGA is a linear amphiphilic copolymer of hydrophobic lactides/hydrophilic glycolides, and widely used to deliver biomedical drugs due to its good mechanical properties, low toxicity, and structural amorphousness

Abbreviations: DSC, dye-sensitized solar cell; PGE, polymer gel electrolyte; APGE, amphiphilic polymer gel electrolyte; PLGA, poly(lactic acid-co-glycolic acid); FTO, fluorine-doped tin oxide; EIS, electrochemical impedance spectroscopy; TEM, transmission electron microscope; VTF, Vogel–Tammann–Fulcher; J_{sc}, short-circuit current density; V_{oc}, open-circuit voltage; *FF*, fill factor; *F*, the Faraday constant; D_i, the diffusivity of species *i*; $c_i(\infty)$, the concentration of species *i* in bulk; δ_i, the diffusion layer thickness; v, the particle velocity; η, the solvent viscosity; ε, dielectric constant; *E*, the magnitude of the applied electric field; ζ, the zeta potential of particles; k_r, the rate constant of the recombination; c_{ox}, the concentration of oxidant (I_3^-); n_0, the electron population in the TiO_2 conduction band in the dark; *n*, the electron population in the TiO_2 conduction band in the light; *p*, the orders of the reaction for I_3^-; *q*, the orders of the reaction for the electrons; σ, the conductivity of the electrolyte; *A*, a pre-exponential factor; *B*, a constant related to the critical free volume for ion transporting; T_0, a reference temperature at which the structural relaxation of solvent becomes zero; T_g, the glass transition temperature.

* Corresponding author. Tel.: +82 54 2792265; fax: +82 54 2798619.
E-mail address: srhee@postech.ac.kr (S.-W. Rhee).

0378-7753/$ – see front matter © 2011 Elsevier B.V. All rights reserved.
doi:10.1016/j.jpowsour.2011.08.053

(low-crystallinity) [30]. Thus, it is expected that the PLGA-based PGE enables high ionic conduction and robustness of DSCs. Furthermore, PLGA is a thermoplastic which turns to the liquid phase near its glass-transition temperature in the range of 40–60 °C and it will show a liquid-like behavior at the operation temperature of DSCs. It will lead to complete wetting of the TiO_2 film and fast diffusive ion-transporting apart from any loss of the solvent and salts. The newly developed APGE not only resolves the problems of liquid electrolytes but also provides deep understanding of the polymeric effects on the cell performance.

2. Experimental details

2.1. Materials

Acetonitrile, tert-butyl alcohol, iodine (I_2), and 4-tert-butylpyridine were purchased from Aldrich, and used without any further purification. 1-Butyl-3-methylimidazolium iodide (BMII) was supplied commercially by Tokyo Chemical Industry (TCI), and used as received. Poly (lactic acid-co-glycolic acid) with the composition rate of 50:50 and the weight-average molecular weight of 20,000 g mol^{-1} (PLGA-5020, Laboratory Grade) was purchased from Wako, Japan. TiO_2 nanocrystal pastes (Ti-Nanoxide T20/SP), cis-diisothiocyanato-bis(2,2′-bipyridyl-4,4′-dicarboxylato) ruthenium(II) bis (tetrabutyl-ammonium) (N719), and transparent conducting glass (FTO glass) substrates with a sheet resistance of 11 Ω $square^{-1}$ were purchased from Solaronix SA, Switzerland. Titanium (IV) oxide anatase nanopowder ca. 25 nm for the ζ-potential measurement and the transmission electron microscopy (TEM) images was obtained from Aldrich, and cleaned by 5 M NaOH and 5 M HNO_3 prior to use.

2.2. Preparation of mesoporous TiO_2 films

The FTO glass substrate was cut into 1.5 cm × 1.25 cm pieces and cleaned ultrasonically with deionized water, ethanol, and acetone. Subsequently, a mesoporous TiO_2 film with the thickness of ca. 15 μm was prepared on the substrate by screen-printing four times, where each step of printing includes relaxation for 3 min to reduce the surface irregularity and drying at 120 °C for 7 min. The film was then sintered at 500 °C for 30 min to remove any residual dispersant. For efficiency measurements, the resulting transparent film was subsequently placed in a 0.02 M aqueous solution of $TiCl_4$ for 12 h at room temperature, and baked once again at 500 °C for 30 min. After cooling down to 80 °C, the TiO_2 film was immersed in a 0.3 mM N719 dye solution in a mixture of acetonitrile and tert-butyl alcohol (vol. ratio, 1:1) and kept at room temperature for 24 h to assure complete adsorption of the sensitizer.

2.3. Preparation of the APGE

0.6 M BMII and 0.06 M I_2 were dissolved into 20 ml acetonitrile and subsequently a certain amount of PLGA (0 wt% for the liquid electrolyte) was added to the mixture. The mixture was stirred overnight at 50 °C under argon atmosphere to form a homogeneous and viscous APGE. Prior to use, the routine additive 0.5 M 4-tert-butylpyridine (tBP) was added to the APGE.

2.4. Assembly of DSCs and symmetric cells

The counter electrode was prepared by thermal platinization (Platisol, Solaronix) of the FTO glass substrate at 400 °C for 15 min, and then assembled with the TiO_2 photoelectrode. For symmetric Pt thin-layer cells, two identical platinized electrodes were used. For both the DSC and the symmetric cell, two electrodes were separated by a 60 μm-thick hot-melting squared frame with a 1.5 mm-wide strip (Surlyn SX 1170, Solaronix), and sealed up by heating at 120 °C. The internal space between the electrodes was filled with the APGE at 50 °C through the electrolyte-injection holes drilled in the counter electrode. The holes were afterward sealed with a Surlyn sheet and a thin glass cover by heating.

2.5. Measurements

The photovoltaic characterization of the DSCs was carried out by a digital source meter (Keithley 2400) under AM 1.5 simulated illumination from a 300 W xenon lamp (Newport 92251A). The diffusive current plateaus for the symmetric Pt cells were obtained by the same device without illumination. The incident light intensity was calibrated by using a standard reference silicon solar cell (PV Measurement Inc.). The electrochemical impedance spectroscope (EIS) measurements were performed by Biologic SP-200 in the frequency range of 100 mHz to 100 kHz at open-circuit voltage. Electrokinetic ζ-potential of the TiO_2 nanoparticle and conductivity of the APGE were measured by Zetasizer Nano ZS90 (Malvern) equipped with the reusable Dip Cell. The hydrogen ion concentration measurements were performed by Orion pH Meter (Thermo) with the Ag/AgCl electrode. The viscosity of the APGE was measured by DV-II Pro viscometer (Brookfield). TEM images of the TiO_2 nanoparticles-PLGA composite were obtained using Hitachi H-7650 with the accelerating voltage of 120 kV.

3. Results and discussion

3.1. Mass-transfer plateaus from the symmetric cells

In an electrochemical system, electric current is controlled by both reaction kinetics and mass transfer. The reaction kinetic-controlled region can be characterized by current densities growing exponentially as a function of potential. On the other hand, the mass transfer-controlled region manifests itself as current density plateaus independent of potential. The mass transfer-limited current density can be obtained in terms of the bulk concentration and diffusivity of the limiting reactant as [31]

$$I_{\lim} = \frac{-nFD_i c_i(\infty)}{\delta_i} \quad (1)$$

where n is the number of electrons transferred, F is the Faraday constant, D_i is the diffusivity of species i, $c_i(\infty)$ is the concentration of species i in bulk, and δ_i is the diffusion layer thickness. In Fig. 1a, the mass transfer control (plateau) of the Pt thin-layer symmetric cells intensifies, i.e., the mass transfer-limited current density decreases, as the PLGA content increases. One should note that the polymer concentration ($\sim 10^{-4}$ M) can be negligible compared with the ion concentration in bulk ($\sim 10^{-2}$ M). Then, the ion concentration in the electrolyte is now assumed constant, and the only variable in Eq. (1) is the diffusivity, D_i. Thus, we concluded that the polymer molecules should hinder the ion transport throughout the medium. The 40 wt% APGE shows the mass transfer-limited current density of ca. 15 mA cm^{-2}, which is 60% of the value obtained in the liquid electrolyte at the same voltage. Fig. 1b shows that the resistance of the arcs in the low frequency range (the Nernst diffusion impedance) increases proportional to the PLGA content, which coincides with the results obtained above.

3.2. Effects of PLGA on J_{sc} and V_{oc} in the APGE-based DSCs

Fig. 2 shows the short-circuit current densities (J_{sc}) and open-circuit voltages (V_{oc}) of the full cells with the APGE for different PLGA contents under simulated AM 1.5 illumination. The APGEs used here contain no intercalative alkali cation such as Li^+, Na^+, and K^+ in order to suppress any alternation in J_{sc} and V_{oc} due to

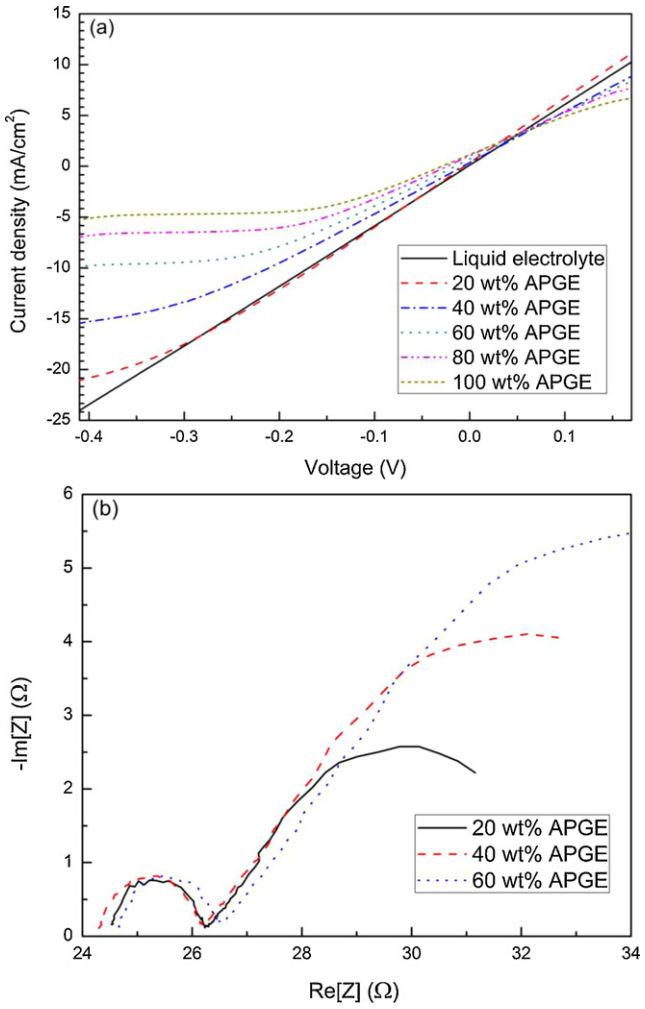

Fig. 1. Effect of the PLGA content on (a) the diffusive current plateaus and (b) the impedance spectra of the symmetric Pt thin-layer cells.

the adsorbed cations on the TiO_2 surface [32]. Interestingly, both J_{sc} and V_{oc} of the APGE show a quite different behavior from the typical PGEs reported in previous researches [4–10,33]. Nevertheless the ionic conductivity of the APGE decreases as the PLGA content

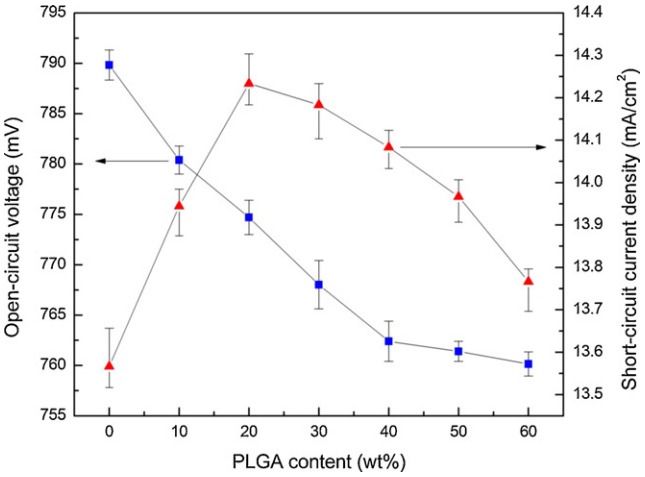

Fig. 2. J_{sc} and V_{oc} of the DSCs with APGE for different PLGA contents under simulated AM 1.5 illumination. The concentrations of BMII and I_2 are 0.6 and 0.06 M, respectively. The data for each point are collected from 10 respective samples.

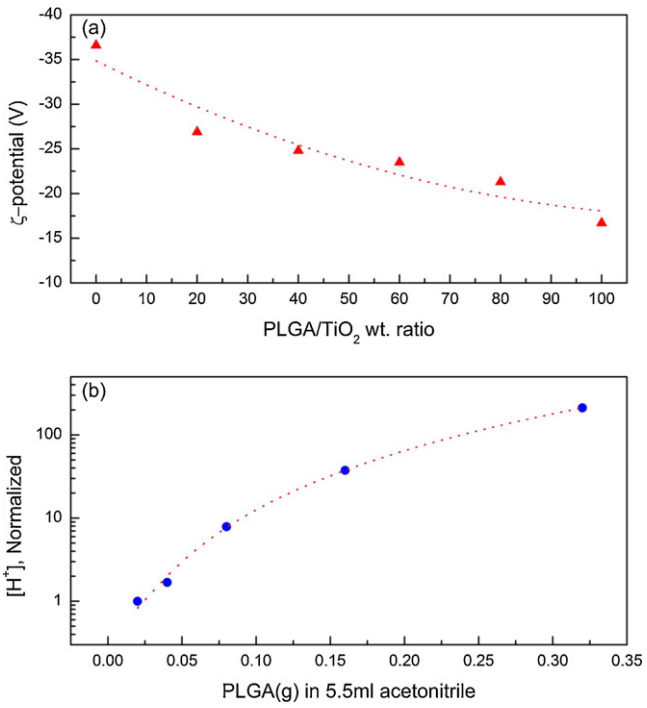

Fig. 3. Effect of the PLGA content on (a) electrokinetic ζ-potential of undyed TiO_2 nanoparticles dispersed in acetonitrile, and (b) hydrogen ion concentrations (normalized) of the PLGA solution in acetonitrile.

increases, J_{sc} increases with the increase of the PLGA content and then gradually decreases after reaching a maximum for 20 wt%. On the other hand, V_{oc} undergoes an exponential decrease as the PLGA content increases. Under the condition of the high I^- concentration used in this study, the effect of PLGA on the redox potential is negligible so that the decrease in V_{oc} infers a shift of the TiO_2 conduction band edge downward with respect to the vacuum level. The downward band-edge shift leads to high electron-injection potential and low recombination rate, resulting in the increase of J_{sc} [34]. For the PLGA content less than 20 wt%, the effects of the band-edge shift dominate over the additional diffusion resistance induced by the polymer molecules and J_{sc} increases. However, the polymeric diffusion resistance becomes substantial at the PLGA contents higher than 20 wt% and limits the current flow to reduce J_{sc} gradually even when V_{oc} decreases. Thus, PLGA has two competitive effects on the magnitude of J_{sc}: one is the downward shift of the TiO_2 conduction band edge and the other is the induction of the additional diffusion resistance.

3.3. Origin of lowering V_{oc} with the increase of the PLGA content

Electrophoretic measurements were carried out to elucidate the interaction of PLGA with the TiO_2 nanoparticles. The ζ-potential of the particle can be determined using the Henry equation

$$\zeta = \frac{3\nu\eta}{2\varepsilon E f(\kappa a)} \quad (2)$$

where ν is the particle velocity, η is the solvent viscosity, ε is its dielectric constant, E is the magnitude of the applied electric field, and $f(\kappa a)$ is a function in which value lies between from 1 to 1.5 depending on the particle radius (a) and the ionic strength of the electrolyte [32,35]. In Fig. 3a, the ζ-potential of the TiO_2 surface undergoes an exponential decrease with the increase in the PLGA/TiO_2 weight ratio and shows consistency with the decay of V_{oc} in Fig. 2. Furthermore in Fig. 3b, the hydrogen ion concentration of the PLGA solution in acetonitrile increases in proportional to the

PLGA concentration. Thus, we concluded that the positive shift of the TiO_2 band edge is ascribed to the adsorption of the hydrogen ions dissociated from PLGA on the TiO_2 surface [36].

It was reported in the past that the positive shift of the band edge by the protonation of TiO_2 decreases V_{oc} [37], but improves J_{sc} with greater electron injection yield [37–39] and higher charge collection efficiency [40]. The yield of electron injection from the excited dyes into TiO_2 is governed by the potential difference between the lowest unoccupied molecular orbital (LUMO) level of the excited dye and the TiO_2 band edge. The driving potential for the electron injection increases with the positive shift of the TiO_2 band edge, and thus the electron injection yield becomes greater to result in high J_{sc}. Besides, the positive charges adsorbed on the TiO_2 surface can compensate the injected electrons to improve the charge collection efficiency so that high J_{sc} can be attained likewise in this case.

3.4. Elongation of the electron life time in the presence of PLGA

EIS measurements of the APGE-based DSCs for some different PLGA contents were carried out in the dark under different forward biases each of which was the same as V_{oc} of the corresponding cell. Kern et al. [41–43] verified that the electron lifetime is inversely proportional to the characteristic frequency at which a peak in low-frequency regime is shown. In Fig. 4, the characteristic frequency increases with the decrease in the PLGA content, i.e., the electron lifetime is elongated in the presence of a large amount of the polymer molecules. Under this condition, the concentration of the recombinative I_3^- ions is lowered by the polymer molecules and thereby the recapture of photoelectrons is suppressed by Eq. (3) [44],

$$J_r = ek_r c_{ox}^p (n^q - n_0^q) \tag{3}$$

where k_r is the rate constant of the recombination, c_{ox} is the concentration of I_3^-, n_0 is the electron population in the TiO_2 conduction band in the dark (n in the light), and the exponents p and q are the orders of the reaction for I_3^- and the electrons, respectively. The TEM images in Fig. 5 show that the polymer molecules tend to adsorb onto the negative TiO_2 surface rather than disperse in the solvent owing to their partially positive ester carbons. Thus, it is concluded that the adsorbed polymer molecules block the interfacial reaction between I_3^- ions and electrons in TiO_2 to eventually increase the electron lifetime.

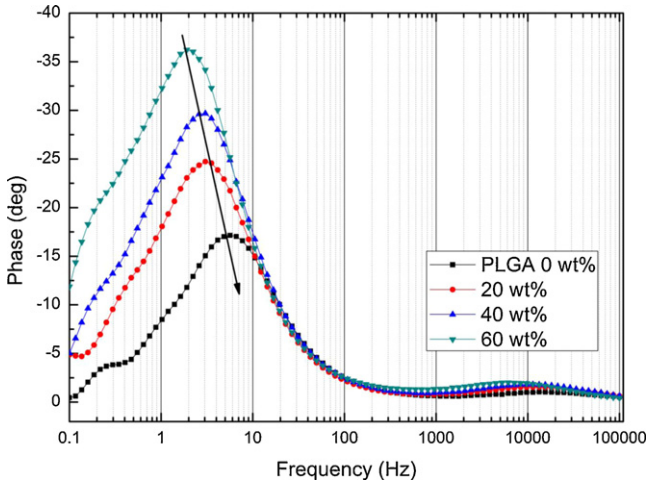

Fig. 4. Effect of the PLGA content on the impedance spectra in Bode phase plots for the APGE-based DSCs. The arrow indicates the shift of the low-frequency peaks with the increase in the concentration.

3.5. Conductivity of the APGE

The Vogel–Tammann–Fulcher (VTF) equation correlates the free volume of the solvent and the conductivity when the ion transport is dominated by the mobility of the solvent molecule [45–47].

$$\sigma = AT^{-1/2} \exp\left[\frac{-B}{T - T_0}\right] \tag{4}$$

where σ is the conductivity, A is a pre-exponential factor, B is a constant related to the critical free volume for ion transporting, and T_0 is a reference temperature at which the structural relaxation of solvent becomes zero, i.e., the glass transition temperature T_g. The conductivity–temperature data in the VTF coordinates are shown in Fig. 6 and clear linear correlations are obtained for both liquid electrolyte and APGE. The glass transition temperatures extracted from the data are 133 and 172 K for the liquid electrolyte and the 40 wt% APGE, respectively. Such low T_g for the APGE indicates the amorphous and low-crystalline nature of the PLGA-based polymer gel. Thus, the APGE can show high conductivities of 10 mS cm^{-1} at 25 °C and 13 mS cm^{-1} at 50 °C.

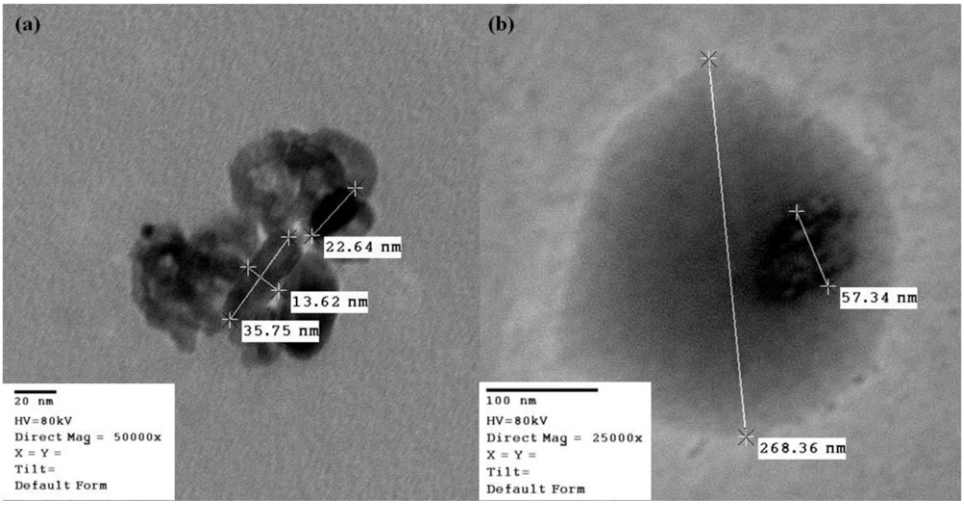

Fig. 5. TEM images of (a) bare TiO_2 nanoparticles dispersed in acetonitrile and (b) the TiO_2 nanoparticle-PLGA mixture in the same solvent.

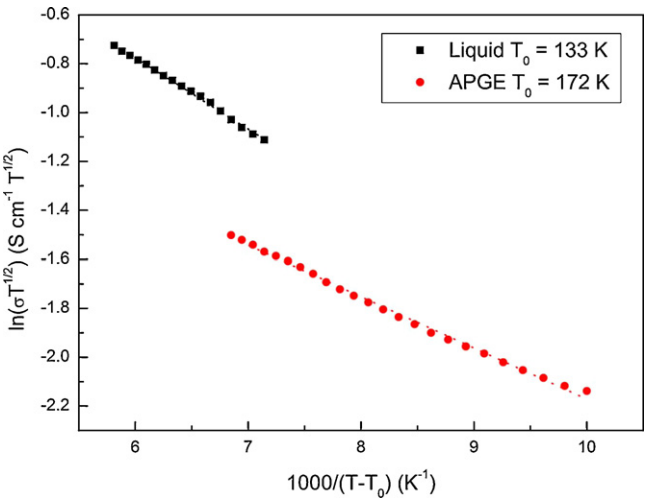

Fig. 6. Vogel–Tammann–Fulcher plots for the liquid electrolyte and the 40 wt% APGE. The reference temperatures (T_0) are extracted from the corresponding conductivity–temperature data and the coefficients of determination (adjusted R^2) of the linear regression for the liquid and the APGE are 0.9970 and 0.9964, respectively.

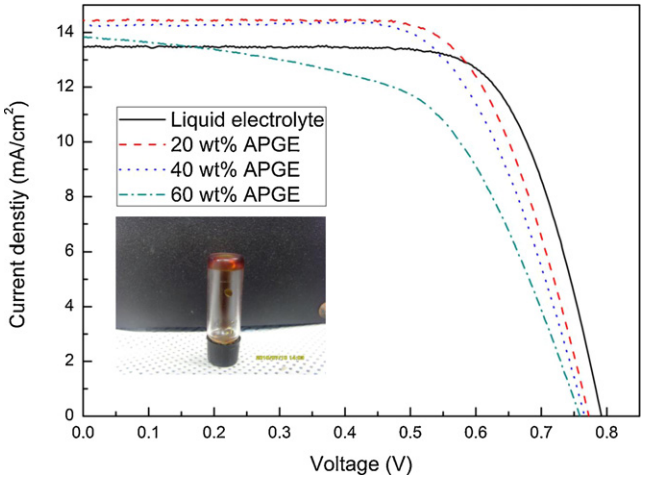

Fig. 7. The current–voltage characteristics of the liquid electrolyte and APGE-based DSCs under irradiation of AM 1.5 simulated sunlight (100 mW cm^{-2}). The inset is a photograph of the 40 wt% APGE which shows that the formed gel did not flow from the top at 5 °C.

3.6. Performance of the APGE-based DSCs

The APGEs contain 20, 40, and 60 wt% PLGA as their polymeric host, respectively. It is found in Fig. 7 that 20 and 40 wt% APGEs can maintain their current level higher than the liquid electrolyte in the low voltage region. It is unprecedented that the PGE containing more than 20 wt% polymer shows higher J_{sc} than the liquid electrolyte. This can be ascribed to the high ionic conductivity of the APGE and the downward shift of the TiO_2 band edge by PLGA as previously described in this study. Table 1 lists the photovoltaic parameters of the liquid electrolyte and APGE-based DSCs. The V_{oc} values of the APGE-based DSCs are slightly inferior to that of the liquid electrolyte-based one, which offsets the high J_{sc} values to yield overall efficiency of 7.5 and 7.4% for 20 and 40 wt% APGE, respectively. Here, the 40 wt% APGE is chosen for further analysis because of high stability and suitable viscosity for practical applications. Due to its thermoplasticity, the APGE becomes viscous liquid (1.21 mPa s at 50 °C) over the temperature range from 30 to 60 °C. It can help ion transporting and penetration of the APGE into the TiO_2 film.

Table 1
The performance of the DSCs with different types of electrolyte. The active area of the cell is 0.25 cm^2 and the irradiation intensity is 100 mW cm^{-2}.

Electrolyte	V_{oc} (mV)	J_{sc} (mA cm^{-2})	FF (%)	η (%)
Liquid	793	13.5	71.5	7.6
20 wt% APGE	772	14.4	68.1	7.5
40 wt% APGE	765	14.2	66.9	7.4
60 wt% APGE	759	13.8	56.8	6.0

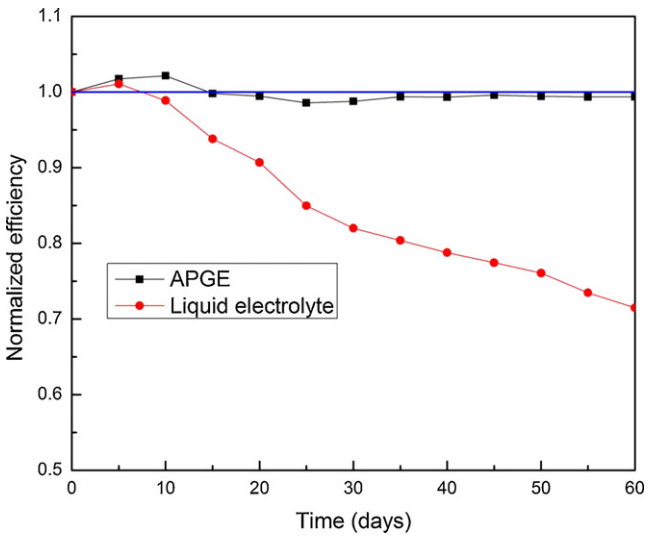

Fig. 8. Normalized efficiencies for the DSCs with the liquid electrolyte and the 40 wt% APGE as a function of time.

3.7. Long-term stability

The APGE-based DSC guarantees long-term stability compared with liquid electrolyte-based one, as shown in Fig. 8. The cells used in this experiment are kept in outside under ambient conditions. The overall efficiency is measured once per week and normalized with respect to that obtained in the first day. During 60 days for the APGE, the overall efficiency lies in ±5% of the initial value, whereas for the liquid electrolyte, the efficiency decreases by 30% mainly due to leakage of volatile solvents. In the beginning 10 days, the efficiency of the DSC with the APGE slightly increases due to further penetration of the APGE into the porous TiO_2 film. The long-term stability is gained by the high polymer concentration of 40 wt%. A larger amount of polymer molecules can provide more "cages" for solvent molecules to be confined. Furthermore, the hydrophilic glycolide groups on the polymer molecule can hold tightly the polar solvent molecules by the van der Waals attraction. Thus, any loss of the solvent can be highly suppressed by the APGE.

4. Conclusion

In this study, we have demonstrated that the novel APGE using PLGA as a polymeric host can make up several disadvantages of the current liquid electrolytes without severe degradation in the photoelectric conversion performance. Long-term stable quasi-solid-state DSCs can be obtained by using the APGE, and they show high photovoltaic conversion efficiency of 7.5 and 7.4% for 20 and 40 wt% APGE, respectively, under AM 1.5 simulated sunlight. The APGE endows with higher J_{sc} than the liquid electrolyte, which attributes to such high performance comparable to typical liquid-state DSCs. In the aspect of the stability, the 40 wt% APGE-based DSC maintained 95% of the initial performance after 60 days in practical conditions. Furthermore, the quasi-solid nature of the APGE may

impart flexibility to DSCs so that some large-scale productions such as roll-to-roll process can be realized. We hope that our findings should deepen understanding of the effects of polymer molecules on the cell performance and provide a guide to developing a suitable PGE for the widespread application of DSCs.

Acknowledgements

This research was supported by the Korea Research Foundation (KRF) through the National Research Laboratory Project and Polymer Gel Cluster group of the Korean government (RT1-04-04-04). The authors thank Hyemin Kim and Sang-Jun Park, POSTECH, for their technical assistance and the availability of the experimental instruments.

References

[1] B. O'Regan, M. Grätzel, Nature 353 (1991) 737–740.
[2] D. Cahen, G. Hodes, M. Grätzel, J.F. Guillenoles, I. Riess, J. Phys. Chem. B 104 (2000) 2053–2059.
[3] M. Grätzel, J. Photochem. Photobiol. A 164 (2004) 3–14.
[4] F. Cao, G. Oskam, P.C. Searson, J. Phys. Chem. 99 (1995) 17071–17073.
[5] W. Cubo, K. Murakoshi, T. Kitamura, S. Yoshida, M. Haruki, K. Hanabusa, H. Shirai, Y. Wada, S. Yanagida, J. Phys. Chem. B 105 (2001) 12809–12815.
[6] P. Wang, S.M. Zakeeruddin, J.E. Moser, M.K. Nazeeruddin, T. Sekiguchi, M. Grätzel, Nat. Mater. 2 (2003) 402–407.
[7] L. Wang, S. Fang, Y. Lin, X. Zhou, M. Li, Chem. Commun. (2005) 5687–5689.
[8] J.H. Wu, Z. Lan, J.M. Lin, M.L. Huang, S.C. Hao, T. Sato, S. Yin, Adv. Mater. 19 (2007) 4006–4011.
[9] J. Wu, S. Hao, Z. Lan, J. Lin, M. Huang, Y. Huang, L. Fang, S. Yin, T. Sato, Adv. Funct. Mater. 17 (2007) 2645–2652.
[10] J. Shi, S. Peng, J. Pei, Y. Liang, F. Cheng, J. Chen, ACS Appl. Mater. Interfaces 1 (2009) 944–950.
[11] U. Bach, D. Lupo, P. Comte, J.-E. Moser, F. Weissörtel, J. Salbeck, H. Spreitzer, M. Grätzel, Nature 395 (1998) 583–585.
[12] Y. Saito, N. Fukuri, R. Senadeera, T. Kitamura, Y. Wada, S. Yanagida, Electrochem. Commun. 6 (2003) 71–74.
[13] J. Krüger, R. Plass, M. Grätzel, P.J. Cameron, L.M. Peter, J. Phys. Chem. B 107 (2003) 7536–7539.
[14] J. Xia, N. Masaki, M. Lira-Cantu, Y. Kim, K. Jiang, S. Yanagida, J. Am. Chem. Soc. 130 (2008) 1258–1263.
[15] B. O'Regan, D.T. Schwartz, Chem. Mater. 10 (1998) 1501–1509.
[16] B. O'Regan, F. Lenzmann, R. Muis, J. Wienke, Chem. Mater. 14 (2002) 5023–5029.
[17] H.J. Lee, P. Chen, S.-J. Moon, F. Sauvage, K. Sivula, T. Bessho, D.R. Gamelin, P. Comte, S.M. Zakeeruddin, S.I. Seok, M. Grätzel, M.K. Nazeeruddin, Langmuir 25 (2009) 7602–7608.
[18] P. Wang, S.M. Zakeeruddin, J.-E. Moser, M. Grätzel, J. Phys. Chem. B 107 (2003) 13280–13285.
[19] P. Wang, S.M. Zakeeruddin, J.-E. Moser, R. Humphry-Baker, M. Grätzel, J. Am. Chem. Soc. 126 (2004) 7164–7165.
[20] D. Kuang, C. Klein, Z. Zhang, S. Ito, J.-E. Moser, S.M. Zakeeruddin, M. Grätzel, Small 3 (2007) 2094–2102.
[21] D. Kuang, P. Wang, S. Ito, S.M. Zakeeruddin, M. Grätzel, J. Am. Chem. Soc. 128 (2006) 7732–7733.
[22] Y. Bai, Y. Cao, J. Zhang, M. Wang, R. Li, P. Wang, S.M. Zakeeruddin, M. Grätzel, Nat. Mater. 7 (2008) 626–630.
[23] W. Kubo, Y. Makimoto, T. Kitamura, Y. Wada, S. Yanagida, Chem. Lett. 31 (2002) 948–949.
[24] S. Anandan, S. Pitchumani, B. Muthuraaman, P. Maruthamuthu, Sol. Energy Mater. Sol. Cells 90 (2006) 1715–1720.
[25] T. Stergiopoulos, I.M. Arabatzis, G. Katsaros, P. Falaras, Nano Lett. 2 (2002) 1259–1261.
[26] G. Katsaros, T. Stergiopoulos, I.M. Arabatzis, K.G. Papadokostaki, P. Falaras, J. Photochem. Photobiol. A 149 (2002) 191–198.
[27] J. Wu, S. Hao, Z. Lan, J. Lin, M. Huang, Y. Huang, P. Li, S. Yin, T. Sato, J. Am. Chem. Soc. 130 (2008) 11568–11569.
[28] Y. Zhou, W. Xiang, S. Chen, S. Fang, W. Zhou, J. Zhang, Y. Lin, Electrochim. Acta 54 (2009) 6645–6650.
[29] J. Barthel, H.J. Gores, G. Schmeer, Ber. Bunsenges. Phys. Chem. 83 (1979) 911–920.
[30] K.Y. Cho, C.H. Kim, J.W. Lee, J.K. Park, Macromol. Rapid Commun. 20 (1999) 598–601.
[31] M.E. Orazem, B. Tribollet, Electrochemical Impedance Spectroscopy, John Wiley & Sons, New Jersey, 2008, p. 79.
[32] S. Pelet, J.-E. Moser, M. Grätzel, J. Phys. Chem. B 104 (2000) 1791–1795.
[33] A.R.S. Priya, A. Subramania, Y.-S. Jung, K.-J. Kim, Langmuir 24 (2008) 9816–9819.
[34] N. Kopidakis, N.R. Neale, A.J. Frank, J. Phys. Chem. B 110 (2006) 12485–12489.
[35] B.J. Kirby, E.F. Hasselbrink Jr., Electrophoresis 25 (2004) 187–202.
[36] D. Kim, H. El-Shall, D. Dennis, T. Morey, Colloid Surf. B 40 (2005) 83–91.
[37] D.F. Watson, G.J. Meyer, J. Coord. Chem. Rev. 248 (2004) 1391–1406.
[38] P. Qu, G.J. Meyer, Langmuir 17 (2001) 6720–6728.
[39] Y. Tachibana, S.A. Haque, I.P. Mercer, J.E. Moser, D.R. Klug, J.R. Durrant, J. Phys. Chem. B 105 (2001) 7424–7431.
[40] D.F. Watson, A. Marton, A.M. Stux, G.J. Meyer, J. Phys. Chem. B 107 (2003) 10971–10973.
[41] R. Kern, R. Sastrawan, J. Ferber, R. Stangl, J. Luther, Electrochim. Acta 47 (2002) 4213–4225.
[42] Q. Wang, J.-E. Moser, M. Grätzel, J. Phys. Chem. B 109 (2005) 14945–14953.
[43] M. Adachi, M. Sakamoto, J. Jiu, Y. Ogata, S. Isoda, J. Phys. Chem. B 110 (2006) 13872–13880.
[44] S.Y. Huang, G. Schlichthörl, A.J. Nozik, M. Grätzel, A.J. Frank, J. Phys. Chem. B 101 (1997) 2576–2582.
[45] M.H. Cohen, D. Turnbull, J. Chem. Phys. 31 (1959) 1164–1168.
[46] G. Adam, J.H. Gibbs, J. Chem. Phys. 43 (1965) 139–146.
[47] G.Y. Gu, S. Bouvier, C. Wu, R. Laura, M. Rzeznik, K.M. Abraham, Electrochim. Acta 45 (2000) 3127–3139.